Proton resonances in ^{24}Mg from $E_x = 12.7$ to 15.7 MeV

J. R. Vanhoy, E. G. Bilpuch, and C. R. Westerfeldt
Duke University, Durham, North Carolina 27706
and Triangle Universities Nuclear Laboratory, Duke Station, Durham, North Carolina 27706

G. E. Mitchell
North Carolina State University, Raleigh, North Carolina 27695
and Triangle Universities Nuclear Laboratory, Duke Station, Durham, North Carolina 27706
(Received 11 May 1987)

The ^{23}Na(p,p$_0$), (p,p$_1$), (p,α_0), and (p,α_1) differential cross sections were measured in the energy range $E_p = 1.08-4.15$ MeV with an overall resolution of 400 eV full width at half maximum. Resonance parameters were obtained for 94 levels with a multilevel, multichannel R-matrix code; parameters include resonance energy, total angular momentum, proton and alpha partial widths, and channel spin and orbital angular momentum mixing ratios. The observed proton and alpha resonance widths provide an upper limit for ^{12}C + ^{12}C reaction rates for an energy region where there are no direct measurements.

I. INTRODUCTION

A series of high resolution proton resonance measurements on odd-mass targets in the 2s-1d shell is in progress at the Triangle Universities Nuclear Laboratory (TUNL). Due to experimental and analysis difficulties there was little spectroscopic information from proton-induced reactions for such targets prior to the present series of measurements. The analysis of these data is much more difficult than analysis of data on zero-spin targets; complications include channel spin and orbital angular momentum mixing, several strongly contributing particle channels, and many levels with a wide range of widths. The even N and Z compound systems formed (^{24}Mg, ^{28}Si, ^{32}S) are well studied by a variety of other reactions, while for the compound systems with odd N and Z (^{26}Al, ^{30}P, ^{34}Cl) there is little available data except from proton transfer reactions. Spectroscopic information on these nuclei is of interest for many reasons. For example, the $T=1$ particle-hole ($f_{7/2}d_{5/2}^{-1}$) states in ^{28}Si were observed as resonances in the ^{27}Al (p,p) reaction, including the 6^- stretched state.[1] A search is underway for states with α_0 decays and large l mixing in the proton channel. The large l mixing would increase the sensitivity of tests of time reversal invariance through detailed balance measurements of (p,α) and (α, p) reactions through the same nuclear resonance. Other reaction cross sections are of particular astrophysical interest. Reactions connecting *sd* shell nuclei are of importance in the energy generation and element production during the carbon, oxygen and silicon burning stages of stellar evolution. In addition to the published results[1-4] on ^{29}Si, ^{27}Al, and ^{25}Mg, we plan measurements on ^{31}P, ^{33}S, ^{35}Cl, and ^{39}K. The present paper reports results for ^{23}Na.

In the present experiment the ^{23}Na (p,p$_0$), (p,p$_1$), (p,α_0), and (p,α_1) channels were measured from $E_p = 1.08$ to 4.15 MeV. The experimental status was summarized by Endt and Van der Leun[5] in 1978. There has been little new information since that compilation; in fact most of the relevant results are in their earlier compilations.[6,7] An investigation by Baumann *et al.*[8] located 36 resonances in the energy range $E_p = 0.58-1.50$ MeV. Luukko *et al.*[9] measured 16 (p, α_0) angular distributions in the range $E_p = 0.59-1.81$ MeV and determined energies and spin assignments, as well as channel spin and orbital angular momentum mixing ratios. Meyer *et al.*[10] determined the energies and strengths of 25 resonances in the (p,γ), (p,p$_1\gamma$) and (p,$\alpha_1\gamma$) channels. The only relevant alpha particle measurement is by Fifield *et al.*:[11,12] a study of the (α,α_0) and (α,$\alpha_1\gamma$) reactions on ^{20}Ne determined spins and decay widths for 54 natural parity states in the excitation energy range 11.86 to 14.33 MeV in ^{24}Mg. This region corresponds to proton bombarding energies of $E_p = 0.17-2.75$ MeV.

The measurement of proton-induced reactions up to 4 MeV on ^{23}Na should add significantly to the available spectroscopic information. This excitation region in ^{24}Mg corresponds to an energy range for ^{12}C+^{12}C fusion which has not been studied. With the proton and alpha resonance partial widths, one can determine an upper limit for the ^{12}C+^{12}C reaction cross section needed for astrophysical reaction rates.

In Sec. II the experimental procedure is described briefly. The resonance analysis is discussed in Sec. III and the data are presented in Sec. IV. In Sec. V the resonance parameters are compared with previous work and the spectroscopic results discussed. The astrophysical implications are considered in Sec. VI and the results are summarized in Sec. VII.

II. PROCEDURE

The experiment was performed with an upgraded model KN Van de Graaff accelerator and associated high resolution system.[13-15] All of the data was measured twice. The first experiment was performed with

five Si surface barrier detectors at laboratory angles of 90°, 108°, 135°, 150°, and 165°. In the second experiment transmission detectors were used to distinguish the α_1 group from protons; the detectors cleanly separated the proton and alpha peaks for beam energies above 2.3 MeV. The final data were obtained with four surface barrier detectors at 90°, 125°, 145°, and 165° and three transmission detectors at 105°, 120°, and 150°. Solid angles of the surface barrier detectors were adjusted such that the Rutherford scattering count rate was approximately the same for all detectors.

Targets consisted of 1–3 μg/cm^2 of Na. The vacuum evaporation was performed with sodium trititanate ($Na_2Ti_3O_7$) in an open tantalum boat. Very little titanium was observed on the targets. The sodium was evaporated onto gold coated ($\sim$1 μg/cm^2) carbon foils ($\sim$5 μg/cm^2). In practice the gold was essential to the preparation of thicker and more stable targets. Typical beam currents were 2 μA, with the integrated beam current adjusted to provide 1–2 % counting statistics.

Our method[14] for obtaining good beam energy resolution uses a control (HH^+) beam to generate a signal to correct for time-dependent energy fluctuations, while the H^+ beam is used to perform the experiment. The HH^+ beam is bent through an electrostatic analyzer, and a correction signal is generated to keep the HH^+ beam fixed in position (and therefore in energy). This signal is suitably amplified and applied to the target. The target potential changes with time to correct for energy fluctuations. In practice targetry effects are very important, and the overall energy resolution function is determined empirically by fitting resonance data. The beam energy is increased automatically,[15] with the voltage on the plates of the electrostatic analyzer changed by a preset amount. Data were taken in energy steps of 100 eV on narrow resonances (sometimes 50 eV) and 400 eV away from resonances.

The spectra were monitored on line and recorded for later analysis. The heart of the data acquisition system is a VAX 11/750 computer, which utilizes the XSYS operating system.[16] The charged particle spectra were analyzed to obtain the yields from the ^{23}Na

TABLE I. Allowed channels for resonances in ^{24}Mg. The final state spins and parities are $\frac{3}{2}^+$ (p_0), $\frac{5}{2}^+$ (p_1), 0^+ (α_0), and 2^+ (α_1). An asterisk indicates the decay is forbidden.

	p_0		p_1		α_0		α_1	
J^π	l	s	l	s	l	s	l	s
0+	2	2	2	2	0	0	2	2
0−	1	1	3	3	*	*	*	*
1+	0	1	2	2	*	*	2	2
	2	1	2	3				
	2	2						
1−	1	1	1	2	1	0	1	2
	1	2	3	2			3	2
	3	2	3	3				
2+	0	2	0	2	2	0	0	2
	2	1	2	2			2	2
	2	2	2	3				
2−	1	1	1	2	*	*	1	2
	1	2	1	3			3	2
	3	1	3	2				
	3	2	3	3				
3+	2	1	0	3	*	*	2	2
	2	2	2	2				
			2	3				
3−	1	2	1	2	3	0	1	2
	3	1	1	3			3	2
	3	2	3	2				
			3	3				
4+	2	2	2	2	4	0	2	2
			2	3				
4−	3	1	1	3	*	*	3	2
	3	2	3	2				
			3	3				
5−	3	2	3	2	5	0	3	2
			3	3				

(p,p_0), (p,p_1), (p,α_0), and (p,α_1) reactions and the ^{197}Au (p,p_0) reaction. Absolute energy calibration was performed with "secondary standard" elastic scattering resonances which have been measured relative to the "primary standard" neutron thresholds for ^{7}Li(p,n) and ^{13}C(p,n) at $E_p = 1.8806$ and $E_p = 3.2357$ MeV.[17]

III. RESONANCE ANALYSIS

The experimental excitation functions were fit with the multilevel, multichannel R-matrix program MULTI6, which is based on the formalism of Lane and Thomas.[18] A best visual fit is obtained by varying the angular momentum, resonance energy, parity, and magnitudes and signs of allowed reduced width amplitudes. All decay channels are fit simultaneously. A description of the fitting procedure for nonzero spin targets is given by Nelson *et al.*[19] Here the analysis procedure is briefly summarized.

For ^{23}Na up to $E_p \sim 4$ MeV the significant particle decay channels are p_0, p_1, α_0, and α_1. The spins and parities of the final states are ^{23}Na (ground state; $J^\pi = 3/2^+$), ^{23}Na ($E_1 = 0.440$ MeV; $J^\pi = \frac{5}{2}^+$), ^{20}Ne (ground state; $J^\pi = 0^+$), and ^{20}Ne ($E_1 = 1.633$ MeV; $J^\pi = 2^+$). The Q value for the ^{23}Na (p,α_0) reaction is $+2.377$ MeV.

The allowed channels for resonances formed by protons on ^{23}Na are listed in Table I. The channel spin is the sum of the intrinsic spins of the ejectile and the residual nucleus. Elastic scattering l values are limited to 4 or less by penetrability considerations; no $l = 4$ proton strength was observed. The l values for alpha decay are limited to $l \leq 5$. Note that for proton elastic and inelastic scattering both channel spin (s) mixing and orbital angular momentum (l) mixing are allowed in general. The α_0 data are extremely important in determining resonance spins (only natural parity states decay through the α_0 channel) and entrance channel mixing ratios.

The channel spin mixing ratios are defined for the nth proton decay channel as

$$\xi_n = \sum_l \Gamma_{p_n, s_>, l} / \Gamma_{p_n} ,$$

where $s_>$ is the higher channel spin and Γ_{p_n} is the total proton width in the nth decay channel. The l-mixing ratios are defined as

$$\tan\psi_{ns} = \pm(\Gamma_{p_n, s, l+2} / \Gamma_{p_n, s, l})^{1/2} .$$

A similar l-mixing ratio can be defined for the α_1 channel. The range of ξ is from 0 to 1, and the range of ψ is from $-90°$ to $+90°$.

Due to very small penetrabilities for higher l values, l mixing is not observed at lower energies. At higher energies l mixing is observed, but the lower l values dominate (on the average) by the ratio of the l and $l+2$ penetrabilities. The l-mixing ratios were determined only for proton elastic scattering. In contrast, channel spin mixing is not dominated by kinematic effects; s-mixing ratios were determined (for elastic scattering) over the entire energy range. The mixing ratios for inelastic scattering are difficult to determine with the present data. More detailed (p,p') angular distributions should assist in selecting among possible solutions for the exit channel mixing. Extensive catalogs of the dependence of resonance shapes and α_0 angular distributions on s mixing and l mixing were generated to aid in the fitting procedure.

The (p,α_0) reaction angular distributions may be used to determine the entrance channel mixing ratios. The normalized Legendre coefficients for $J^\pi = 1^-$, 2^+, and 3^- resonances are

$$(1^-)\quad a_2 = -(1-\xi) + \tfrac{1}{5}\xi\cos^2\psi_2 + \tfrac{4}{5}\xi\sin^2\psi_2 - \tfrac{3}{5}\sqrt{6}\xi\sin(2\psi_2)\cos(\phi_1-\phi_3) ;$$

$$(2^+)\quad a_2 = \tfrac{5}{7}(1-\xi) - \tfrac{15}{49}\xi\sin^2\psi_2 - (\tfrac{10}{7})^{1/2}\xi\sin(2\psi_2)\cos(\phi_0-\phi_2) ,$$

$$a_4 = -\tfrac{12}{7}(1-\xi) + \tfrac{36}{49}\xi\sin^2\psi_2 ;$$

$$(3^-)\quad a_2 = (1-\xi) + \tfrac{4}{5}\xi\cos^2\psi_2 + \tfrac{19}{45}\xi\sin^2\psi_2 - \tfrac{4}{5}(\tfrac{3}{7})^{1/2}(1-\xi)\sin(2\psi_2)\cos(\phi_1-\phi_3) ,$$

$$a_4 = \tfrac{3}{11}(1-\xi) - \tfrac{9}{11}\xi\sin^2\psi_2 - 2(\tfrac{3}{7})^{1/2}\xi\sin(2\psi_2)\cos(\phi_1-\phi_3) ,$$

$$a_6 = \tfrac{125}{99}\xi\sin^2\psi_2 - \tfrac{25}{11}(1-\xi) .$$

The subscript $n = 0$ has been suppressed. Since l mixing can occur only for $s = 2$ for these cases (see Table I), only ψ_2 appears. The ϕ's are energy dependent phase shifts, including both Coulomb and hard sphere phases.

In the final fit the contributions from all resonances and all channels were included. Reduced widths in channel c are defined by $\gamma_c^2 = \Gamma_c / 2P_c$, where the Coulomb penetrability is calculated from the Coulomb wave function evaluated at a channel radius $R_c = 1.25(1 + A^{1/3})$ fm.

IV. RESULTS

Experimental data were obtained up to $E_p = 4.15$ MeV. Above $E_p = 3.5$ MeV there are many large overlapping resonances, and reliable parameters could not be extracted for all resonances. A complete analysis is presented only for the region $E_p = 1.08$–3.50 MeV. The resonance parameters listed are the best choice considering data from both experimental runs and at all detector angles.

The (p,p_0) data are shown at 165° in Figs. 1–3. The (p,p_1) data are also shown up to 2.7 MeV (Figs. 1 and 2). Above 2.7 MeV the p_1 group was obscured by the carbon elastic scattering group. The α_1 channel was weaker at lower energies and was not resolved from the proton groups between $E_p = 1.6$ and 2.3 MeV because of characteristics of the transmission detector employed. The (p,α_1) data are therefore available only above 2.3 MeV (Figs. 2 and 3). The (p,α_0) data were obtained throughout the entire energy region.

Due to difficulty in obtaining uniform targets, the quality of these data is not as high as that we obtained on the neighboring nuclei ^{27}Al and ^{29}Si. In addition, the analysis was extremely difficult due to the presence of many very large resonances. These two effects led to poorer large scale agreement between the R-matrix fit and the data than we obtained for other nuclei. In almost all cases the resonances parameters (E_0, J, π, Γ_p, Γ_α) are still well determined, but the uncertainties in the mixing parameters are larger than in previous analyses. A major concern is the possibility of systematic error. Analysis of data at several angles and independent tests for target stability indicate no significant target deterioration. Fits to the p_0 data below 1.2 MeV at all angles are systematically low. This suggests problems with target uniformity, which are accentuated by the rapid changes in the beam optics at low energies. At higher energies, for example near $E_p = 1.6$ and 2.8 MeV, the apparent disagreement is probably due to very broad resonances. We prefer not to list such resonances without stronger evidence. Even with these limitations the data provide a large amount of new information: they are the only data for proton-induced resonance reactions above $E_p = 1.8$ MeV.

The resonance parameters are listed in Table II for the p_0, p_1, α_0, and α_1 channels. Typical uncertainties in the widths are ±10% for laboratory widths less than a few keV, and ±20% for large widths (tens of keV). In Table II the laboratory widths are listed for a given l and s; the l-mixing and s-mixing ratios can be easily obtained from this information. In some cases the resonance shapes are very insensitive to the s-mixing ratio. Uncertainties in s-mixing ratios are strongly l and J dependent: ~25% for $l = 1$ and ~50% for $l = 2$. Typical uncertainties for l-mixing angles are ~10°.

Previous experimental work on these reactions was summarized in Sec. I. There is excellent agreement for the 16 resonances below $E_p = 1.51$ MeV with J^π assignments given in the 1973 compilation by Endt and Van der Leun.[6] The widths agree qualitatively. The present resonance energies average about 4 keV lower for 20 corresponding resonances in the compilation with widths

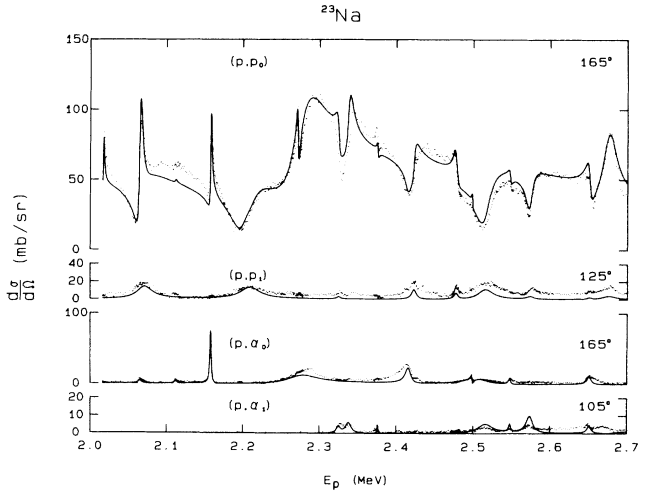

FIG. 2. ^{23}Na(p,p_0), (p,p_1), (p,α_0), and (p,α_1) differential cross sections in the energy range $E_p = 2.00$–2.70 MeV. The solid line is the R-matrix fit to the data.

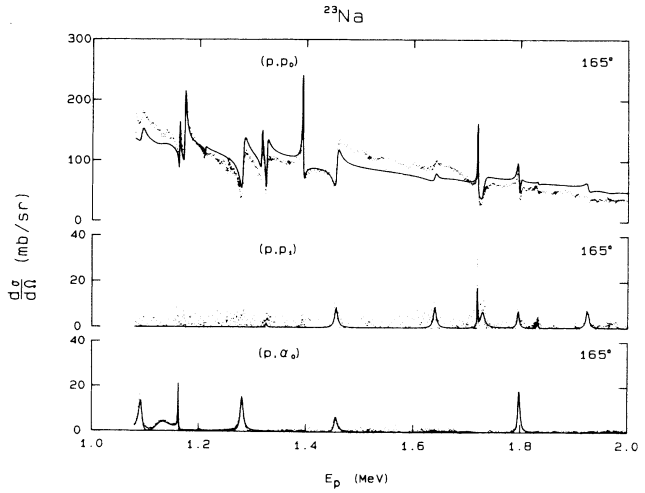

FIG. 1. ^{23}Na(p,p_0), (p,p_1), and (p,α_0) differential cross sections in the energy range $E_p = 1.08$–2.00 MeV. The solid line is the R-matrix fit to the data.

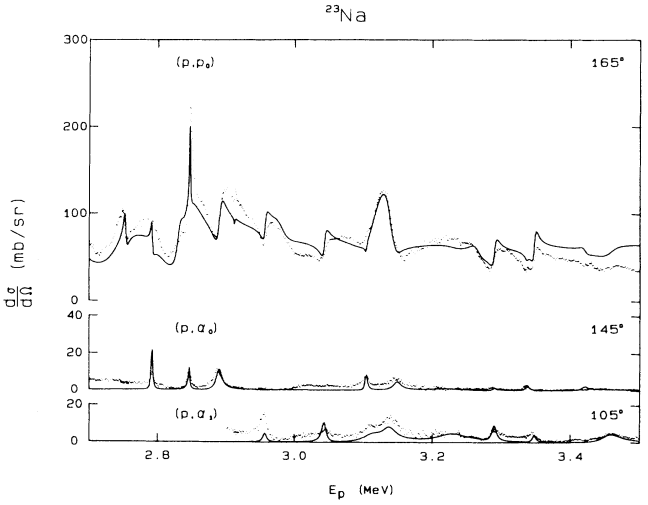

FIG. 3. ^{23}Na(p,p_0), (p,α_0), and (p,α_1) differential cross sections in the energy range $E_p = 2.70$–3.50 MeV. The (p,p_1) reaction in this energy range is obscured by proton scattering from carbon. The solid line is the R-matrix fit to the data.

TABLE II. Resonance parameters for ^{23}Na(p,X). One asterisk means that both values of channel spin give equivalent fits. Two asterisks denote decay observed, but not analyzed.

		(p,p$_0$)				(p,p$_1$)[a]				(p,α_0)			(p,α_1)		
E_p (MeV)	J^π	l	s	Γ^b (keV)	γ^2 (keV)	l	s	Γ^b (keV)	γ^2 (keV)	l	Γ^b (keV)	γ^2 (keV)	l	Γ^b (keV)	γ^2 (keV)
1.087	2^+	0	2	+0.9	11					2	+7.0	34			
		2	2	−0.08	39										
1.128	2^+	0	2	0.8	13					2	30	130			
1.1591	2^+	0	2	+0.3	2.7					2	−0.8	2	0	0.3	34
1.1691	1^+	0	1	2.8	24										
1.2055	2^-	1	1	0.008	0.2								1	0.3	140
		1	2	0.012	0.32										
	$(1)^-$	1	*	0.04	1.0								1	0.3	140
	$(3)^-$	1	2	0.015	0.40								1	0.3	140
1.2073	(0^-)	1	1	1	28										
1.2507	1^+	0	1	0.035	0.24								2	0.29	58
	$(2)^+$	0	2	0.015	0.10								2	0.25	50
1.2781	3^-	1	2	6	120	1	*	0.1	21	3	0.55	5.6			
1.3136	1^+	0	1	2.0	11	2	*	0.05	100						
		2	1	0.4	69										
1.322	2^-	1	1	1.0	35	1	*	0.15	23				1	0.075	18
		1	2	2.0	18										
1.3907	2^+	0	2	0.4	150										
		2	1	1.4	38										
1.407[c]								**							
1.4540	3^-	1	2	5.5	65	1	2	0.3	21	3	0.25	1.8			
		3	2	−0.25	500	1	3	0.3	21						
1.498[c]	$(0^+,2^+,3^-)$										**				
1.549[c]	$(0^+,2^+,3^-)$							**			**				
1.567[c]	(1^-)										**				
1.633	1^-	1	1	4.5	33					1	40	41			
1.639	$(1)^+$	0	1	2.25	5.9	2	*	2.4	750						
		2	1	1.35	75.5										
1.709	1^-	1	1	1.0	6.3					1	−25	23			
		1	2	0.2	1.3										
1.7186	3^+	2	1	0.43	19	0	3	0.3	2						
		2	2	0.43	19										
1.7277	2^-	1	1	5.75	34	1	2	1.5	32						
		1	2	1.75	10										
1.7951	$(1)^+$	2	1	3.5	130	2	*	0.8	120						
	$(2)^+$	2	1	2.5	91	0	*	2	11						
1.7978	3^-	1	2	+3.5	18					3	+0.75	2.9			
		3	2	+0.2	110										
1.8312	2^+	2	*	0.1	0.7	0	2	2	10						
	$(1)^+$	2	*	0.5	3.3	2	3	3	14						
1.925	$(1)^+$	2	*	1.5	40	2	3	5.5	21						
	$(2)^+$	2	*	0.9	24	2	3	5	19						
	$(3)^+$	2	*	0.5	13	2	3	4.5	17						
1.969	$(1)^-$	1	*	3	11					1	30	21			
2.0182	1^+	0	1	1.0	1.5										
		2	2	0.5	11										
	$(1)^+$	0	1	1.0	1.5										
		2	1	0.4	8.6										
2.066	2^+	0	2	+4.0	5.6					2	+0.3	0.32			
		2	1	+0.8	5.8										
2.072	2^-	1	1	8	26	1	2	15	120						
2.113	2^+	0	2	0.2	0.26					2	2.2	2.3			
		2	*	0.2	3.5										
2.1594	5^-	3	2	0.7	150					5	1.2	48			
2.202	1^-	1	2	24	54						(**)				
2.212	2^-	1	1	10	26	1	*	10	57						
		1	2	10	26										

TABLE II. (*Continued*).

		(p,p$_0$)				(p,p$_1$)[a]				(p,α_0)			(p,α_1)		
E_p (MeV)	J^π	l	s	Γ^b (keV)	γ^2 (keV)	l	s	Γ^b (keV)	γ^2 (keV)	l	Γ^b (keV)	γ^2 (keV)	l	Γ^b (keV)	γ^2 (keV)
2.274	1^+	2	2	2.0	26										
2.279	2^+	0	2	35	39					2	13	11			
2.327	$(1)^+$	2	*	2	24	2	2	1	30				2	2	28
	$(2)^+$	0	2	0.8	0.85	2	*	1	30				2	2	28
		2	*	2.0	24										
	$(3)^+$	2	*	0.5	5.9	2	*	1	31				2	2	28
2.340	1^+	0	1	6	6.3								2	2	27
2.3785	$(1)^+$	2	*	0.23	2.5								2	2.3	28
	$(2)^+$	2	*	0.14	1.5								2	1.4	17
	$(3)^+$	2	*	0.10	1.1								2	1.0	12
2.419	3^-	1	2	+1.0	2					3	−7.5	11.5			
2.426	2^+	0	2	2	2	2	2	5	120						
2.481	1^+	2	2	2.5	23	2	*	3	64						
2.5021	2^+	2	2	+0.25	2.2					2	+1.0	0.7			
2.51	1^-	1	2	+10	18					1	−20	9			
2.519	3^-	1	2	9	16	1	2	9	30				3	4.5	130
2.5514	2^+	0	2	+0.2	0.18					2	+1	0.7	0	1.0	2.4
		2	2	+0.7	5.8										
2.578	2^-	1	1	3.0	5.2	3	*	1	230				3	3.0	75
		1	2	3.0	5.2										
2.655	4^+	2	2	1.5	8.5	2	*	1	15	4	2.0	7.6	2	2.0	13
2.676	1^+	0	1	20	16	2	*	3	44						
2.75	1^+	0	1	60	46								2	7	35
2.7575	3^+	2	*	1.25	7.7								2	2.0	10
2.7967	$(4)^+$	2	2	0.7	4.1					4	15	4.7			
2.82	0^-	1	1	30	41										
2.837	1^+	0	1	13	9.5										
	$(2)^+$	0	2	13	9.5										
2.848	(2^-)	1	2	20	27										
2.8510	(4^+)	2	2	+0.19	1.0					4	5	15			
		4	2	−0.11	99										
2.8520	3^-	3	2	1.0	51					3	0.5	0.5			
2.896	2^+	0	2	5	3.5					2	5	2.6			
2.9178	(0^-)	1	1	1.0	1.3										
	(1^-)	3	*	0.2	9										
2.9505	J^{nat}										**				
2.9626	2^+	0	2	2	1.4	0	2	2	2				0	2	2.4
2.988	$(0)^+$	2	2	25	115										
3.049[d]	(1^+)	0	1	3.5	2.3								2	3.5	10
3.049[d]	(1^-)	1	2	2	2.3								1	6	9
3.10	(1^-)	1	*	10	11					1	100	32	1	10	14
	(4^+)	2	2	2	8					4	60	130	1	10	14
3.1104	3^-	1	2	+0.4	0.44					3	3	2.5			
		3	2	−0.1	3.4										
3.122	1^+	0	1	25	16								2	8	20
3.144	$(2)^+$	2	1	11	42								2	5	12
		2	2	7	28										
3.154	1^-	1	2	2	2					1	12	3.8			
3.23	1^-	1	1	5	5					1	50	15			
3.24	$(1)^+$	2	1	10	35								2	40	85
3.272	$(0)^+$	2	2	17	58								2	1	2
3.297	2^+	0	2	3	1.7					2	0.5	0.2	0	4.0	3.1
3.345	1^-	1	1	0.6	0.6					1	4	1.2			
		1	2	0.4	0.4										
3.3558	1^+	0	1	5	2.8								2	1.0	1.8
3.428[c]	J^{nat}										**				
3.46	$(1)^-$	1	1	5	4.4					1	75	21			

TABLE II. (*Continued*).

E_p (MeV)	J^π	(p,p$_0$) l	s	Γ^b (keV)	γ^2 (keV)	(p,p$_1$)[a] l	s	Γ^b (keV)	γ^2 (keV)	(p,α_0) l	Γ^b (keV)	γ^2 (keV)	(p,α_1) l	Γ^b (keV)	γ^2 (keV)
3.47	1^+	0	1	8	4.3								2	25	38
	(2^-)	1	*	4	3.4								1	15	13
3.543	1^+	2	2	8	21					2	−1.5	0.5	0	3	2
3.595	1^+	0	1	15	7.6								2	7	9
3.65	2^+	0	1	30	15					2	5	1.7	0	5	2
3.706[c]														**	
3.723	(1^+)	2	2	25	56	2	3	15	9						
3.75[c]														**	
3.775[c]	J^{nat}										**				
3.86[c]															
3.88[c]	J^{nat}										**			**	
3.90	1^+	2	1	50	100								2	10	9
3.97	(4^+)	2	*	1.6	3					4	60	48			
		4	1	0.4	54										
3.98[e]	(1^+)	2	*	+10	18								2	+40	35
4.012[c]														**	
4.05[c]	J^{nat}										**				
4.07[c]														**	
4.083[c]	J^{nat}										**				
4.124[c]	J^{nat}										**				

[a]One possible solution is given. For the p$_1$ channel, the values for l and s are uncertain.

[b]Signs associated with the partial widths indicate the sign of the reduced width amplitude. Only the relative signs between the p$_0$ and α_0 amplitudes are determined; the p$_0$ amplitude with the lowest l value is assumed positive.

[c]Only total widths are determined for the resonances at $E_p=1.407$ MeV (3.7±0.5 keV), $E_p=1.498$ MeV (6±1 keV), $E_p=1.549$ MeV (5.5±0.5 keV), $E_p=1.567$ MeV (3±1 keV), $E_p=4.328$ MeV (10±3 keV), $E_p=3.706$ MeV (< 10 keV), $E_p=3.75$ MeV (38±9 keV), $E_p=3.775$ MeV (12±3 keV), $E_p=3.86$ MeV (80±30 keV), $E_p=3.88$ MeV (22±6 keV), $E_p=4.012$ MeV (< 10 keV), $E_p=4.05$ MeV (< 10 keV), $E_p=4.07$ MeV (65±15 keV), $E_p=4.083$ MeV (24±5 keV), and $E_p=4.124$ MeV (25±10 keV).

[d]A superimposed pair of resonances.

[e]Relative signs of amplitudes with respect to the resonance at $E_p=3.90$ MeV are important.

less than 10 keV in the energy range $E_p=1.09-2.07$ MeV. The origin of this discrepancy is not known. The only major disagreement is for the $\Gamma_T\sim30$ keV d-wave resonance at $E_p=1.136$ MeV. The present 2^+ assignment is supported by the (p,α_0) experiment of Luukko *et al.*[9] There is some confusion concerning the resonance(s) at $E_p=1.278$ MeV. Endt and Van der Leun[6] list this structure as possibly a close doublet. Meyer *et al.*[10] report a state with spin (2^+,3, 4^+) at $E_p=1.2828$ MeV with $\Gamma_T=6.3\pm1.0$ keV. Luukko *et al.*[9] report a 5.2 keV 1^- state at 1.284 MeV. We observe no evidence for two resonances in the p$_0$ and α_0 channels. The α_0 angular distribution is consistent with a single 3^- state. Four resonances with significant p$_1$, α_0, and α_1 widths were not observed in the elastic excitation function. Total widths and possible spin assignments are given as the observed channels permit. The overall agreement with previous measurements is good.

In the region above $E_p=3.5$ MeV there is relatively little structure in the proton channel and the cross section is much smaller. The p$_1$ group is completely engulfed by protons elastically scattered from ^{12}C. The observed resonances have large widths. Although it is impossible to fit all of these higher energy data, parameters were obtained for some of the resonances, primarily from (p,α) data.

V. SPECTROSCOPIC RESULTS

A. Analog states

The $T=1$ analog states in ^{24}Mg may be compared with parent states in ^{24}Na. The location of analog states can be estimated with an average Coulomb energy shift. However, large shifts from this simple prediction occur for the lowest states in the ^{24}Na-^{24}Mg system. We therefore determined an empirical relation from a least-squares fit to 11 analogs previously identified by Schmalbrock *et al.*[20] up to $E_x(^{24}\text{Mg})=12.05$ MeV and $E_x(^{24}\text{Na})=2.562$ MeV. The empirical relation is

$$E_p=1.010E_x(^{24}\text{Na})-2.294\ \text{MeV}\ ,$$

where E_p is the laboratory proton bombarding energy. No information was available on analog states in the energy region of the present experiment; there was also no relevant (^{3}He,d) data. Spectroscopic factors have been determined[21] with the (d,p) reaction for states up to $E_x=4.19$ MeV in ^{24}Na. Only four of these states in ^{24}Na are expected to have corresponding proton widths large enough to be observed in the present experiment. The available transfer data restrict identification of analog states to the region below $E_p=2$ MeV.

The method of identifying analog states and calculat-

ing spectroscopic factors is described by Bilpuch *et al.*[14] Proton single particle widths are estimated following the Zaidi and Darmodjo[22] and Harney[23] method discussed in detail by Harney and Wiedenmüller.[24] In order to compare directly with the neutron transfer results, potential well parameters are those used in the (d,p) analysis[21] and the $2T_0+1$ factor is included in S_p.

(i) The analog of the $E_x = 3.372$ MeV 2^- state in ^{24}Na is expected near $E_p = 1.12$ MeV with $\Gamma_p \sim$ keV. No 2^- resonance was observed in this region.

(ii) The analog of the 3.413 MeV 1^+ state in ^{24}Na is expected near $E_p = 1.16$ MeV with $\Gamma_p \sim 15$ keV. There is a 1^+ resonance at $E_p = 1.1691$ MeV, but the $l=0$ proton spectroscopic factor S_p is only 0.04 compared with $S_{dp} = 0.28$ ($l=0$) and 0.31 ($l=2$). We do not observe the $l=2$ component because of the very low $l=2$ penetrability.

(iii) The analog of the $E_x = 3.589$ MeV 1^+ state in ^{24}Na is expected near $E_p = 1.34$ MeV with $\Gamma_p \sim 2$ keV. The 1^+ resonance at $E_p = 1.3136$ MeV has

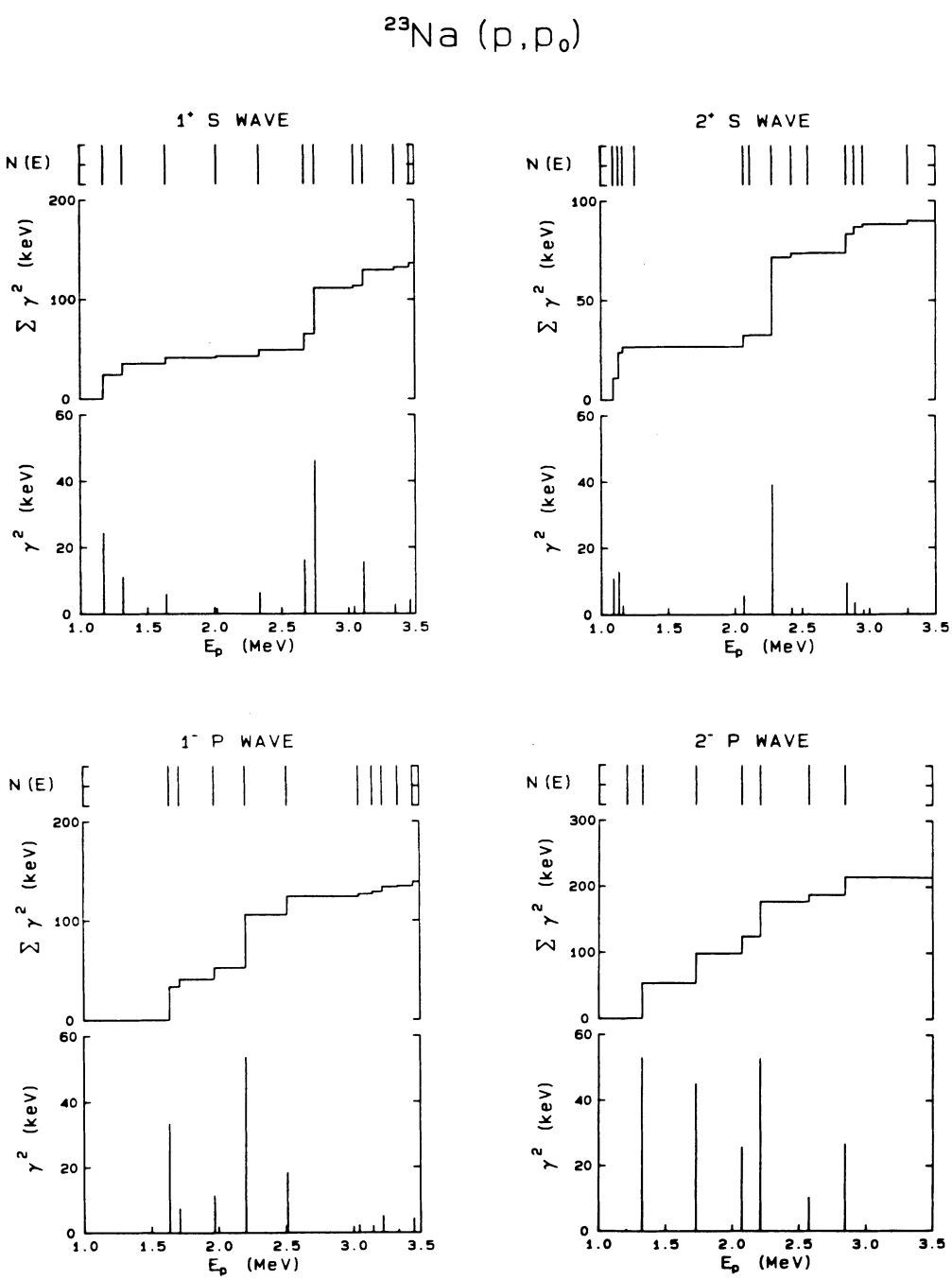

FIG. 4. Level positions and proton reduced widths and sum of reduced widths for 1^+ and 2^+ $l=0$ resonances and 1^- and 2^- $l=1$ resonances in ^{24}Mg. The strengths are summed over channel spin.

$S_p(l=0)=0.02$ and $S_p(l=2)=0.08$, as compared with $S_{dp}(l=0)=0.04$ and $S_{dp}(l=2)=0.12$.

(iv) The analog of the $E_x=4.187$ MeV 2^+ state in ^{24}Na is expected near $E_p=1.95$ MeV. No $l=0$ width was observed for this resonance; the proton spectroscopic factor $S_p(l=2)=0.05$, as compared with $S_{dp}(l=2)=0.04$. The 2^+ assignment for this resonance is tentative.

B. Proton strengths

The proton reduced widths are shown in Figs. 4 and 5 for 1^+, 2^+ $(l=0)$; 1^-, 2^-, 3^- $(l=1)$; 1^+, 2^+ $(l=2)$; and 3^- $(l=3)$ states. For other l, J, and π combinations there are too few states to plot. Since there is no information concerning analogs above $E_p=2$ MeV (no corresponding data on parent states in ^{24}Na), some

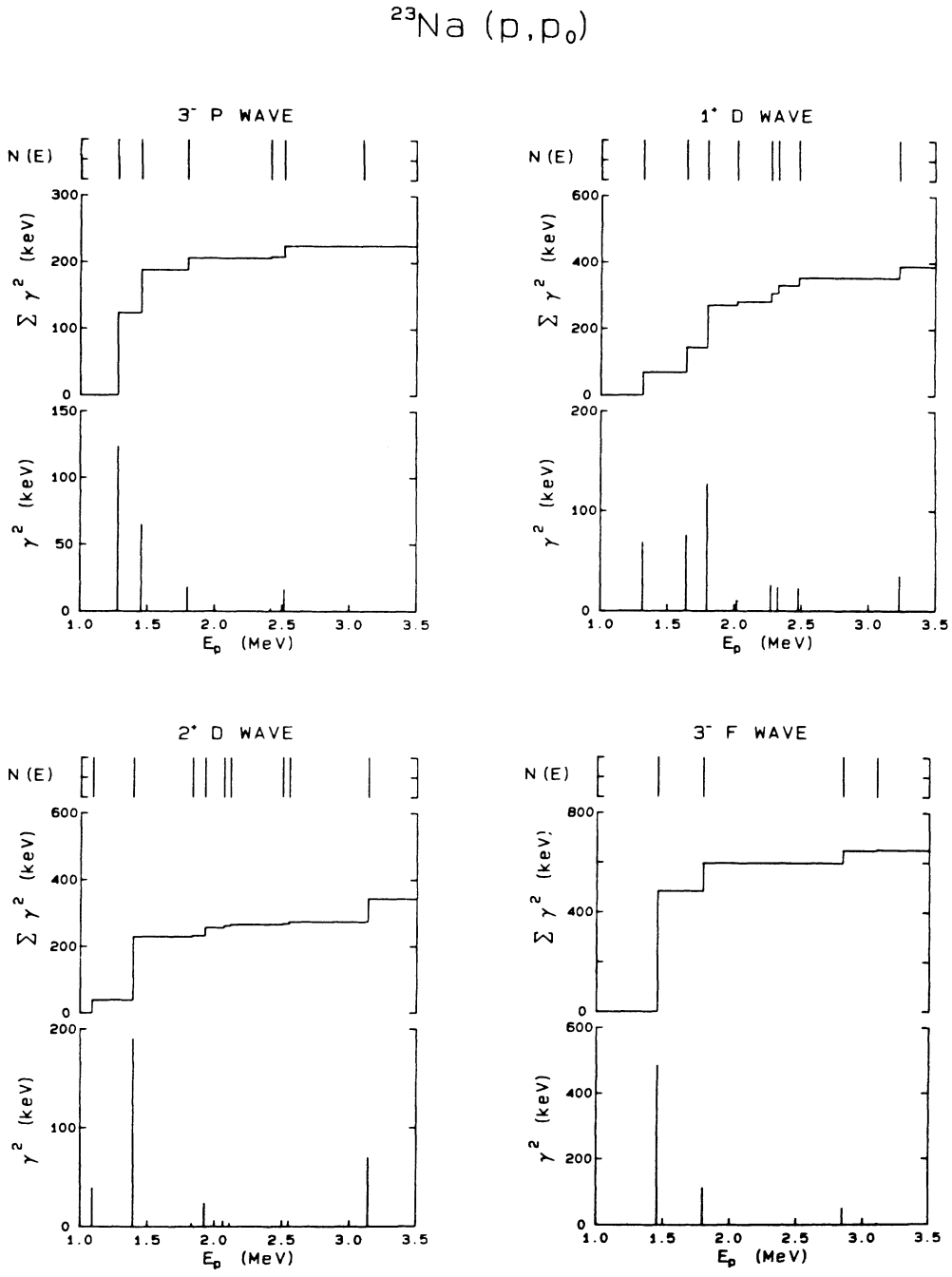

FIG. 5. Level positions and proton reduced widths and sum of reduced widths for 3^- $l=1$ resonances, 1^+ and 2^+ $l=2$ resonances, and 3^- $l=3$ resonances, in ^{24}Mg. The strengths are summed over channel spin.

of the large anomalies (for example, the 1^+ resonance near 2.7 MeV, the 1^- resonance near 2.2 MeV) may be analog states. However, there are also individual states with extremely large reduced widths which are known to be nonanalog states (for example the 3^- state near 1.3 MeV, the 1^+ state near 1.8 MeV and the 2^+ state near 1.4 MeV).

Although the cumulative strengths are large, all are less than half the single particle value except for 3^- $l=3$, for which there is a very large error. The cumulative strengths are listed in Table III. The proton single particle value was obtained with the code HANS;[24] the values obtained (~ 700 keV) are close to the single particle estimate $\gamma^2_{\text{s.p.}} = \hbar^2/2ma^2$. For states which are formed by two channels, we used $2\gamma^2_{\text{s.p.}}$ for the sum rule.

TABLE III. Proton elastic strengths in ^{24}Mg.

J^π	l	Levels	Channels[a]	$\sum\gamma^2$ (keV)	Sum rule (%)
1^+	0	11	1	140	18
2^+	0	13	1	90	12
0^-	1	3	1	70	10
1^-	1	10	2	140	10
2^-	1	7	2	210	15
3^-	1	6	1	230	30
0^+	2	3	1	190	25
1^+	2	8	2	390	26
2^+	2	9	2	340	23
3^+	2	3	2	47	3
4^+	2	4	1	22	3
1^-	3		1		
2^-	3		2		
3^-	3	4	2	650	44
4^-	3		2		
5^-	3	1	1	150	20

[a]Strengths are summed over channel spin. The sum rule limit is the number of channels times the single particle value.

C. Alpha strengths

The α_0 strengths are plotted in Fig. 6 for 1^-, 2^+, and 3^- states. The absolute strengths are smaller than the proton strengths, but the fractions of the sum rule are larger. We adopt the simplest assumption, that the "single particle" value for alphas is $\gamma^2_{\text{s.p.}}(\alpha) = \gamma^2_{\text{s.p.}}$ (p)/4. The cumulative strengths are listed for the α_0 and α_1 decays in Table IV. There is only one decay channel unless there is l mixing, which occurs in practice only for α_1 decay from 2^+ states. For the sum in this case we used twice $\gamma^2_{\text{s.p.}}(\alpha)$. The fraction of the sum rule is greater than 50% for α_0 decay from 1^- and 2^+ states and α_1 decay from 1^+, 2^-, 2^+, and 3^- states. Thus many of the states at this excitation energy in ^{24}Mg have a very large component of an alpha particle coupled to the ground or first excited state of ^{20}Ne.

D. Strength functions

The strength function is defined as $\langle\gamma^2\rangle/\langle D\rangle$. Spin-spin forces in the nucleon-nucleus interaction will result in differences in values for the s-wave strength functions for states of different J. Many neutron s-wave strength functions have been extracted,[25] and in some cases considerable differences were observed for different J values. However, the results are inconclusive due to small sample size (12–50 levels) and to possible intermediate structure effects. Nelson *et al.*[1] measured a strength function ratio $S_{J<}/S_{J>} = 3.5$ for 33 s-wave proton resonances on ^{27}Al. The sample size is similarly restricted in the present experiment (13 1^+ and 12 2^+ levels); the ratio of 1^+ and 2^+ strengths is $S_{J<}/S_{J>} = 0.61 \pm 0.35$. The error quoted is the fractional statistical error, which is $(2/n)^{1/2}$ for a Porter-Thomas distribution.

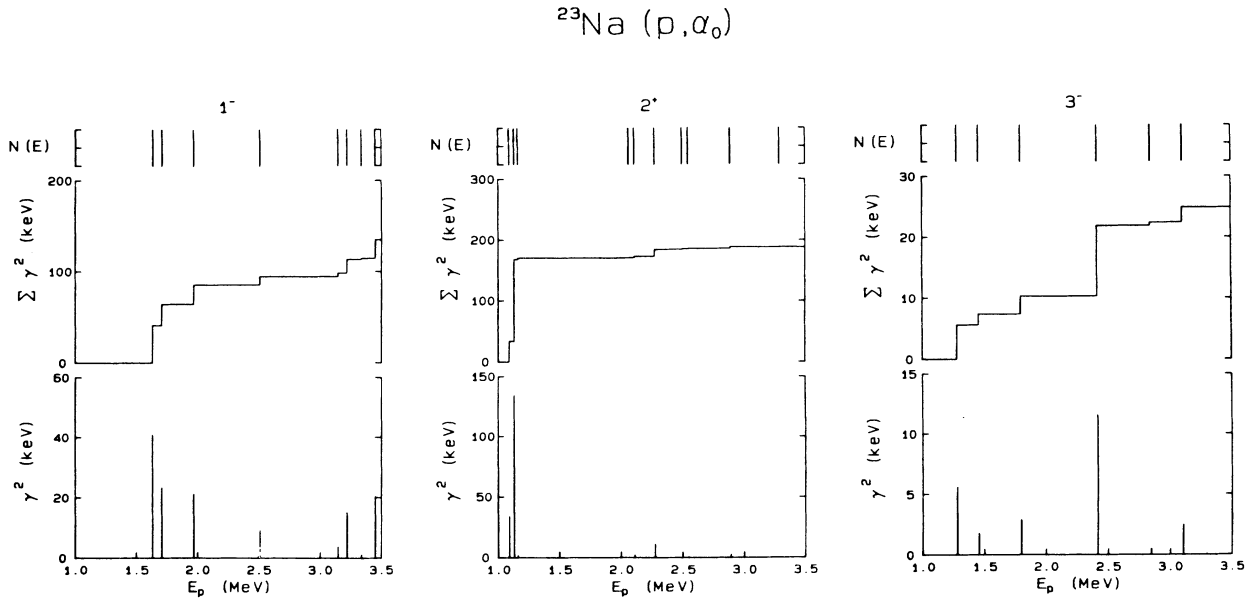

FIG. 6. Level positions and alpha reduced widths and sum of reduced widths for 1^-, 2^+, and 3^- resonances in ^{24}Mg.

TABLE IV. Alpha strengths in ^{24}Mg.

J^π	l	Levels	$\sum\gamma^2$ (keV)	Sum rule (%)
		α_0		
1^-	1	8	140	64
2^+	2	10	190	89
3^-	3	6	25	12
		α_1		
1^-	1	1	8.8	4
1^+	2	8	250	(100)[a]
2^-	1	3	230	(100)[a]
2^+	0+2[b]	6	100	50
3^-	1	1	130	63
3^+	2	2	22	11
4^+	2	1	12	6

[a]Values in excess of the sum rule are obtained with the single particle estimate $\hbar^2/(2ma_c^2)$.

[b]There is only one exit channel unless l is mixed, which occurs only for the α_1 decay from the 2^+ states. Due to the small penetrability, only $l=0$, 1, and 2 are considered for α_1 decay.

Coupling of the nucleon and target spins also may cause dependence of the p-wave strength functions on total angular momentum. Identification of p-wave resonances in proton elastic scattering is much easier than for neutron scattering, due to the strong dependence of the characteristic resonance shapes on l value. The $l=0$, 1, and 2 proton strength functions on zero-spin targets have been measured in the mass range $A\sim 40$–60 at TUNL (Ref. 14) and Tokyo.[26] Unfortunately a quadratic ambiguity occurs when transforming from the channel spin to the angular momentum representation. Thus at present the p-wave strength function data are of no practical value in the search for spin-spin effects.

VI. ASTROPHYSICAL IMPLICATIONS

Understanding nucleosynthesis and energy generation in stars requires a knowledge of many nuclear reactions. In particular, the reactions proceeding through mass 24—^{23}Na(p,α), ^{20}Ne(α,γ) and ^{12}C(^{12}C,X)—provide information on the energy generation during the carbon burning phase of stellar evolution and on the initial abundances for later stages of steller evolution.[27]

Calculation of thermonuclear reaction rates involves the overlap of reaction cross sections with the thermal distribution of velocities,

$$N_A\langle\sigma v\rangle = N_A\int_0^\infty \sigma(E)v\phi(v,T)dv \ \text{cm}^3/\text{s/mole} ,$$

where

$$\phi(v,T)=\left[\frac{m}{2\pi kT}\right]^{1/2} e^{-mv^2/2kT}4\pi v^2 dv .$$

The velocity distribution is taken as Maxwellian at a temperature T_9 in billions of degrees Kelvin ($kT=T_9/11.6$ MeV). Due to the interplay between the reaction cross section and the high energy tail of the Maxwell-Boltzmann distribution, a rather narrow energy range contributes most of the yield. This region is centered at an energy $E_0\cong 0.122(Z_1^2Z_2^2A)^{1/3}T_9^{2/3}$ MeV, with a total width $\Delta E_0\approx 0.237(Z_1^2Z_2^2A)^{1/6}T_9^{5/6}$ MeV.[28] Although the average reaction cross section is governed by the Coulomb barrier penetration probability, the location and spin of resonances can have dramatic effects on the reaction rate. For the compound nuclear processes, the cross section may be taken as a sum of Breit-Wigner contributions.

$$\sigma(E)=\pi\lambda\!\!\!^{-2}\sum\frac{2J+1}{(2i+1)(2I+1)}\frac{\Gamma_{\text{out}}\Gamma_{\text{in}}}{(E_0-E)^2+(\Gamma_T/2)^2} .$$

The reaction rates of Fowler *et al.*[29] for ^{23}Na(p,α) were determined from resonances lying below $E_p\cong 1$ MeV. At temperatures $T_9>1$, resonances above $E_p=1.0$ MeV are the major contributors to the reaction rates. The rates obtained including resonances from the present experiment are compared with the empirical formula of Fowler in Fig. 7. Resonance parameters for $E_p<1.01$ MeV are taken from Kuperus *et al.*[30] ($E_p<500$ keV) and Luukko *et al.*[9] ($0.592<E_p<1.01$ MeV). The present calculation indicates an approximate factor of 10 increase over the empirical formula in the range $1<T_9<6$. For temperatures $T_9\geq 5$, resonances lying above $E_p=4$ MeV (above our measurements) become important contributors to the integral.

In the C+C fusion reaction, the region of interest is $E_{\text{c.m.}}=1.0-5.1$ MeV for $0.3<T_9<3.0$. Almquist *et al.*,[31] Patterson *et al.*,[32] Mazarakis and Stephens,[33] Becker,[34] and Kettner *et al.*[35] have measured the C(C,p) and C(C,α) cross sections down to 2.45 MeV. Measurements of heavy-ion cross sections at low energy are extremely difficult. Often it is sufficient to extrapolate the measured cross sections into the region of interest, but in the case of ^{12}C+^{12}C, large intermediate structure effects are observed. For carbon energies $E_{\text{c.m.}}=0.0$–1.7 MeV the corresponding energy range for protons on ^{23}Na is

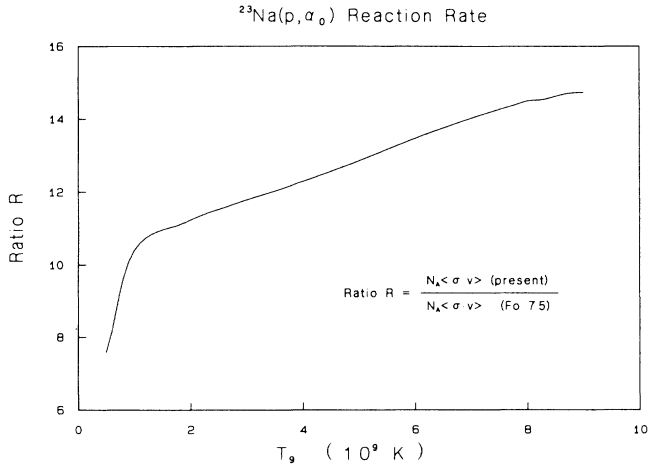

FIG. 7. Temperature dependence of the reaction rate for ^{23}Na(p,α_0). The present results are compared with those calculated by Fowler. See text for discussion.

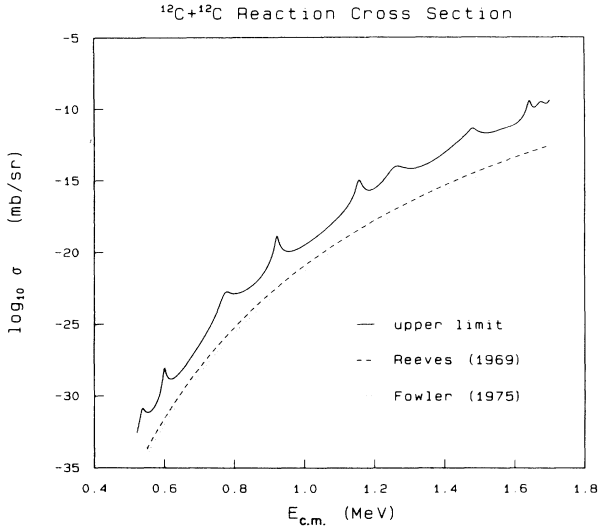

FIG. 8. Carbon-carbon fusion cross sections. The dashed and dotted curves are extrapolations using parameters from Reeves and Fowler, respectively. The solid line is the upper limit for the fusion cross section proceeding through the compound nuclear resonances measured in the ^{23}Na(p,p) and ^{23}Na(p,α) reactions. See text for discussion.

$E_p = 2.3-4.1$ MeV. In the present experiment several resonances are observed in this energy range with large proton and alpha widths.

Although a calculation of the C+C reaction cross section requires a knowledge of the carbon partial widths, an upper limit for the fusion cross section (proceeding through these compound nuclear states) may be obtained by assuming the maximum value allowed for the carbon partial width—a single particle unit [$\gamma^2_{s.p.}$(CC)=105 keV]. Because the entrance channel consists of identical spin zero bosons, only even, natural parity resonances contribute to the cross section. Resonances lying at $E_p = 2.50$ MeV and above were included in the calculation. The carbon channel radius was 5.5 fm. The exit channel widths were taken as the observed total widths. The calculated fusion cross section is shown in Fig. 8. Resonances appear in the rapidly changing cross section, which is dominated by the Coulomb penetrability. The extrapolations of Reeves[36] and Fowler *et al.*[29] are shown for comparison. The parametrization by Reeves is a fit to the $E_{c.m.} = 5$ MeV region of the C+C cross section with the standard form

$$\sigma(E) = \frac{S(E)}{E} e^{-2\pi\eta} e^{-aE},$$

with $S(E)$ set to a constant, S_0. The parametrization by Fowler uses an analytic expression for $S(E)$,

$$S(E) = S_0(e^{-\gamma E^m} + be^{\beta E})^{-1}$$

to fit the available data over a wider range of energies. A different choice for S_0 leads to the difference in the extrapolations of Reeves and Fowler. Of course the spectroscopic factors for decay into the carbon-carbon channel are less than the assumed value of one. Average spectroscopic factors on the order of $10^{-3}-10^{-2}$ produce approximate agreement with the extrapolations of Reeves and Fowler *et al.* It appears that simple compound nucleus processes may be sufficient to explain the extrapolated ^{12}C-^{12}C fusion cross sections near $E_{c.m.} \sim 1$ MeV.

VII. SUMMARY

The ^{23}Na (p,p$_0$), (p,p$_1$), (p,α_0), and (p,α_1) reactions have been measured in the energy range $E_p = 1.08-4.15$ MeV with an overall resolution of 400 eV. Resonance parameters were extracted for 94 levels with a multilevel, multichannel R-matrix code. Two analog states were identified. The ratio of $l=0$ strength functions was measured to be $S_{J=1}/S_{J=2} = 0.61 \pm 0.35$. Very strong α_0 and α_1 decay was observed for many resonances. The astrophysical reaction rates for the ^{23}Na(p,α_0) reaction were obtained for the region above $T_9 = 1$. The ^{12}C-^{12}C reaction rates are not well known in the energy region $E_{c.m.} = 1.0-2.5$ MeV. Proton and alpha widths for even natural parity states were used to provide an upper limit for the ^{12}C-^{12}C fusion cross section through simple compound nucleus processes in a region where there are currently no direct measurements. It would be extremely interesting to look directly at ^{12}C+^{12}C reactions in this energy region.

ACKNOWLEDGMENTS

The authors would like to thank D. P. Balamuth, C. Rolfs and P. M. Endt for valuable discussions. The assistance of R.O. Nelson, B.J. Warthen, W. K. Brooks, and J.S. Bull in performing the experiment is appreciated. This work is supported in part by the U.S. Department of Energy, Office of High Energy and Nuclear Physics, Contract Nos. DE-AC05-76ER01067 and DE-AS05-76ER03624.

[1]R. O. Nelson, E. G. Bilpuch, C. R. Westerfeldt, and G. E. Mitchell, Phys. Rev. C **30**, 755 (1984).
[2]R. O. Nelson, E. G. Bilpuch, C. R. Westerfeldt, and G. E. Mitchell, Phys. Rev. C **27**, 930 (1983).
[3]R. O. Nelson, E. G. Bilpuch, C. R. Westerfeldt, and G. E. Mitchell, Phys. Rev. C **29**, 1656 (1984).
[4]G. Adams, E. G. Bilpuch, G. E. Mitchell, R. O. Nelson, and C. R. Westerfeldt, J. Phys. G **10**, 1747 (1984).
[5]P. M. Endt and C. Van der Leun, Nucl. Phys. **A310**, 1 (1978).
[6]P. M. Endt and C. Van der Leun, Nucl. Phys. **A214**, 1 (1973).
[7]P. M. Endt and C. Van der Leun, Nucl. Phys. **A105**, 1 (1967).
[8]N. P. Baumann, F. W. Prosser, W. G. Read, and R. W. Krone, Phys. Rev. **104**, 376 (1956).
[9]A. Luukko, A. Anttila, M. Bister, and M. Piiparinen, Phys. Scr. **2**, 159 (1970).
[10]M. A. Meyer, J. P. L. Reinecke, and D. Reitmann, Nucl.

Phys. **A185**, 625 (1972).
[11]L. K. Fifield, M. J. Hurst, T. J. M. Symons, F. Watt, C. H. Zimmerman, and K. W. Allen, Nucl. Phys. A **309**, 77 (1978).
[12]L. K. Fifield, M. J. Garman, M. J. Hurst, T. J. M. Symons, F. Watt, C. H. Zimmerman, and K. W. Allen, Nucl. Phys. **A322**, 1 (1979).
[13]C. R. Westerfeldt, G. E. Mitchell, E. G. Bilpuch, and D. A. Outlaw, Nucl. Phys. **A303**, 111 (1978).
[14]E. G. Bilpuch, A. M. Lane, G. E. Mitchell, and J. D. Moses, Phys. Rep. **28**, 145 (1976).
[15]C. R. Westerfeldt, R. O. Nelson, E. G. Bilpuch, and G. E. Mitchell, Triangle Universities Nuclear Laboratory (TUNL) Technical report, 1986 (unpublished).
[16]C. R. Gould, L. G. Holzsweig, S. E. King, Y. C. Lau, R. V. Poore, N. R. Roberson, and S. A. Wender, IEEE Trans. Nucl. Sci. **28**, 3708 (1981).
[17]J. B. Marion, Rev. Mod. Phys. **38**, 660 (1966).
[18]A. M. Lane and R. G. Thomas, Rev. Mod. Phys. **30**, 257 (1958).
[19]R. O. Nelson, E. G. Bilpuch, and G. E. Mitchell, Nucl. Instrum. Methods A **236**, 128 (1985).
[20]P. Schmalbrock, H. W. Becker, L. Buchmann, J. Görres, K. U. Kettner, W. E. Kieser, H. Kräwinkel, C. Rolfs, and H. P. Trautvetter, Nucl. Phys. **A398**, 279 (1983).
[21]C. Daum, Nucl. Phys. **45**, 273 (1963).
[22]S. A. A. Zaidi and S. Darmodjo, Phys. Rev. Lett. **19**, 1446 (1967).
[23]H. L. Harney, Nucl. Phys. **A119**, 591 (1968).
[24]H. L. Harney and H. A. Weidenmüller, Nucl. Phys. **A139**, 241 (1969).
[25]J. E. Lynn, *The Theory of Neutron Resonance Reactions* (Clarendon, Oxford, 1968).
[26]Y. Ozawa and E. Arai, Z. Phys. A **324**, 381 (1986).
[27]C. A. Barnes, S. Trentalange, and S.-C. Wu, in *Treatise on Heavy-Ion Science*, edited by D. A. Bromley (Plenum, New York, 1984), Vol. 6.
[28]D. D. Clayton and S. E. Woosley, Rev. Mod. Phys. **46**, 755 (1974).
[29]W. A. Fowler, G. R. Caughlin, and B. A. Zimmerman, Ann. Rev. Astron. Astrophys. **13**, 69 (1975).
[30]J. Kuperus, P. W. M. Glaudemans, and P. M. Endt, Physica **29**, 1281 (1963).
[31]E. Almquist, J. A. Kuehner, D. McPherson, and W. E. Vogt, Phys. Rev. **136**, B1384 (1964).
[32]J. R. Patterson, H. Winkler, and C. S. Zaidins, Astrophys. J. **157**, 367 (1969).
[33]M. G. Mazarakis and W. E. Stephens, Phys. Rev. C **7**, 1280 (1973).
[34]H. W. Becker, Diplomarbeit, Universität Münster, 1978 (unpublished).
[35]K. U. Kettner, H. Lorenz-Wirzba, and C. Rolfs, Z. Phys. A **298**, 65 (1980).
[36]H. Reeves, Astrophys. J. **146**, 447 (1966).